# Doppler instability of antispiral waves in discrete oscillatory reaction–diffusion media*

Qian Yu(钱 郁), Huang Xiao-Dong(黄晓东), Liao Xu-Hong(廖旭红), and Hu Gang(胡 岗)†

*Department of Physics, Beijing Normal University, Beijing* 100875, *China*

(Received 22 September 2009; revised manuscript received 20 October 2009)

This paper investigates antispiral wave breakup phenomena in coupled two-dimensional FitzHugh–Nagumo cells with self-sustained oscillation via Hopf bifurcation. When the coupling strength of the active variable decreases to a critical value, wave breakup phenomenon first occurs in the antispiral core region where waves collide with each other and spontaneously break into spatiotemporal turbulence. Measurements reveal for the first time that this breakup phenomenon is due to the mechanism of antispiral Doppler instability.

**Keywords:** antispiral waves, break up, Doppler instability
**PACC:** 0545, 0565, 8220M

## 1. Introduction

Spiral wave dynamics has been investigated extensively in a variety of physical, chemical, and biological systems.[1−3] Usually, spiral waves in reaction–diffusion systems rotate outwardly through the medium from the spiral core area. Recently, a new type of inwardly propagating rotating spiral waves (antispiral waves) were numerically revealed[4,5] and experimentally observed by Vanag and Epstein in the oscillatory Belousov–Zhabotinsky (BZ) reaction that dispersed in water droplets of a water-in-oil aerosol OT (AOT) microemulsion (BZ-AOT system).[6−8] This discovery raised great interests in the field of nonlinear dynamics. A series of theoretical and experimental studies have been carried out and the mechanism underlying antispiral wave behaviour has been explained using complex Ginzburg–Landau equation (CGLE) equation and some oscillatory reaction–diffusion systems.[9−14]

Transitions from regular patterns to spatiotemporal chaos in extended systems remain a challenging problem in nonlinear dynamics.[15] In particular spiral wave instability leading to defect turbulence in various systems is a robust phenomenon observed in both experiments and numerical simulations.[16−26] Phenomenologically, two different kinds of spiral wave breakup scenarios have been documented in experiments and numerical simulations: Doppler instability[17−19] and Eckhaus instability.[20−23] The first instability usually occurs in excitable media where spiral waves break up near the spiral core which has been hypothesized to be a mechanism of cardiac fibrillation.[24] In the second instability, which usually appears in oscillatory media, spiral wave breakup happens far from the spiral core, and the region near the core may remain practically unchanged. Recently, Yang *et al.* found Doppler instability in a oscillatory media in the vicinity of saddle-node bifurcation.[26] However, to our knowledge, there is no evidence on whether Doppler instability can appear in the oscillatory media via Hopf bifurcation. For antispiral waves which can happen only in oscillatory media, there have been very few papers addressing the instability problem. Recently, Xie *et al.* studied FitzHugh–Nagumo (FHN) model around a Hopf bifurcation condition, and investigated the Eckhaus instability of antispiral waves.[27] So far, Doppler instability has never been observed in antispiral waves. In this paper, we will focus our investigation on this problem. We will study a two-dimensional (2D) medium of coupled FHN cells to reveal the possibility of Doppler instability of antispiral waves in oscillatory media, and investigate the mechanism and features of this instability.

## 2. Model

The oscillatory system under investigation consists of the following coupled reaction–diffusion

*Project supported by the National Natural Science Foundation of China (Grant No. 10675020) and by the National Basic Research Program of China (973 Program) (Grant No. 2007CB814800).
†Corresponding author. E-mail: ganghu@bnu.edu.cn
© 2010 Chinese Physical Society and IOP Publishing Ltd

equations:[28]

$$\begin{aligned}
\dot{u}_{i,j} &= \frac{1}{\varepsilon}(u_{i,j} - \frac{u_{i,j}^3}{3} - v_{i,j}) + D_{i,j}^u, \\
\dot{v}_{i,j} &= u_{i,j} - \sigma v_{i,j} + \delta + D_{i,j}^v, \\
D_{i,j}^u &= D_u(u_{i-1,j} + u_{i+1,j} + u_{i,j-1} + u_{i,j+1} - 4u_{i,j}), \\
D_{i,j}^v &= \gamma D_u(v_{i-1,j} + v_{i+1,j} + v_{i,j-1} + v_{i,j+1} - 4v_{i,j}),
\end{aligned} \tag{1}$$

where $i = 1, \ldots, N_1$ and $j = 1, \ldots, N_2$. Variables $u_{i,j}$ and $v_{i,j}$ in Eq. (1) are the fast and slow variables, respectively, parameter $\epsilon > 0$ is the ratio of the time scales of the active variable $u$, and the inhibit variable $v$, $\sigma$ and $\delta$ are two other control parameters that determine the number of fixed points, $D_u$ is the spatial coupling strength for the active variable $u$, and $\gamma > 0$ is the ratio of the coupling strength of the inhibit variable $v$ over that of the active variable $u$. For the parameter region $0 < \sigma < 1$, we have a homogeneous fixed point solution $(u_0, v_0)$ and this solution undergoes Hopf bifurcation with a critical parameter at $\epsilon_c = (1 - u_0^2)/\sigma$. Linear stability analysis shows that, if $\epsilon < \epsilon_c$ the fixed point losses its stability via Hopf bifurcation and the system adopts stable limit cycle solution with frequency $\Omega = \sqrt{\sigma/(1 - u_0^2) - \sigma^2}$. In this paper, we fix $\epsilon = 1.20$, $\sigma = 0.5$, $\delta = 0.0$, $\gamma = 2.5$, and vary $D_u$. For infinitely large systems $D_u$ can be scaled to a fixed value (e.g., $D_u = 1$). It is emphasized that $D_u$ is a relevant parameter for the system dynamics for medium with fixed finite size. In particular, when $D_u$ is small there is a nonscaling region for discrete systems where $D_u$ can never be scaled out even for infinite system size. Our work will show the influence of $D_u$ upon the antispiral wave breakup in the following part of this paper. An interesting point is that for a large parameter region of $D_u$ we observe stable antispiral waves, i.e., waves propagate inwardly towards the spiral tip, the wave source. It is the central task of this paper to investigate possible Doppler instability of antispiral waves in discrete oscillatory reaction–diffusion media. With $\sigma = 0.5$ and $\delta = 0.0$, the Hopf bifurcation occurs at $\epsilon_c = 2.0$. Our simulation is taken on a two-dimensional ($2D$) square sheet with $200 \times 200$ ($N_1 = N_2 = 200$) spatial discrete sites and the No-Flux boundary condition is used. Equation (1) is integrated by the second-order Runge–Kutta scheme with the time step $\Delta t = 0.01$. A suitable initial condition is chosen so that only one stable antispiral can be formed in the middle of the square sheet. Then we use this stable antispiral as the initial condition to investigate the instability of antispiral waves in discrete reaction–diffusion media which are oscillatory via Hopf bifurcation.

## 3. Results

As the coupling strength $D_u$ decreases, the dynamical behaviour of the antispiral is changed dramatically. At large coupling strength, we observe periodic and inwardly propagating spiral waves which are completely stable everywhere. The snapshot of $u$ for $D_u = 0.0352$ is shown in Fig. 1(a). A stable antispiral has been formed in the middle of the system. The corresponding space–time plots of $u$ at $y = 100$ in Fig. 1(b) shows that the spiral waves propagate from the boundaries of the medium to the spiral core centre. The corresponding time series and trajectories of the spiral core centre (at the space site (100,100)) and the spiral arm far away from the core centre (at the space site (190,100)) are shown in Figs. 1(c) and 1(d) respectively. From these pictures we can see that the spiral core centre is not completely fixed, but oscillates with a small amplitude. And the tip of the antispiral waves follows a small circle, as indicated in Fig. 2(a). Here we define the antispiral tip to be the intersection of the two contours $u = 0.20$ and $f(u = 0.20, v) = 0$, where $f = u - u^3/3 - v$ is the local dynamics of variable $u$. However, when the coupling strength $D_u$ is decreased to the first critical value $D_u^{c_1} \approx 0.0341$, the system undergoes a transition from simple inwardly rotating waves to meandering antispiral waves (compound inwardly rotating spiral waves). Two types of meandering motions in continuous excitable media have been observed in previous works: hypocycloid (outward flower petal) and epicycloid (inward flower petals).[16,18] In our case, the tip of antispiral waves follows a hypocycloid trace, as shown in Fig. 2(b). As we decrease $D_u$ further in the meandering region, more complicated flower petals of the tip trace have been found as shown in Figs. 2(c) and 2(d).

To provide evidence that a supercritical Hopf bifurcation is responsible for the transition indicated in Fig. 2, we compute the amplitude ratio of the two modes of the compound inwardly rotating waves against the parameter distance from the critical point in Fig. 3. The amplitude $r_1$ of the primary mode is the average radius of the petals and the amplitude of the secondary mode reads $r_2 = R/2 - r_1$, where $R$ is the maximum outer diameter of the orbit.[18] Near the bifurcation point, the growth of the secondary mode is given by a power law with exponent $\sim 1/2$.

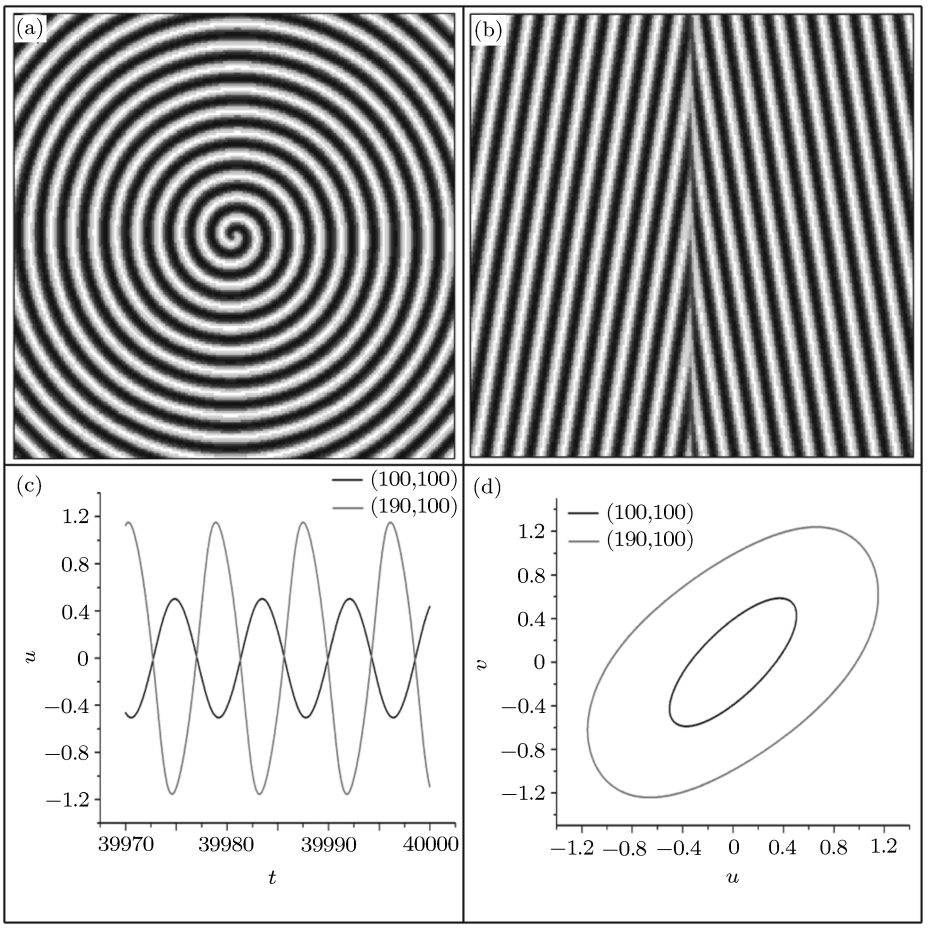



**Fig. 1.** (a) Snapshot of $u$ in the FHN model (1) with $D_u = 0.0352$. (b) Corresponding space–time plots of $u$ at $y = 100$. (c) Time series of $u$ at the space sites (100,100) and (190,100). (d) The corresponding trajectories in $u - v$ plane at the space sites of (c). Parameters $\epsilon = 1.20$, $\sigma = 0.5$, $\delta = 0.0$, $\gamma = 2.5$ are fixed throughout this paper.

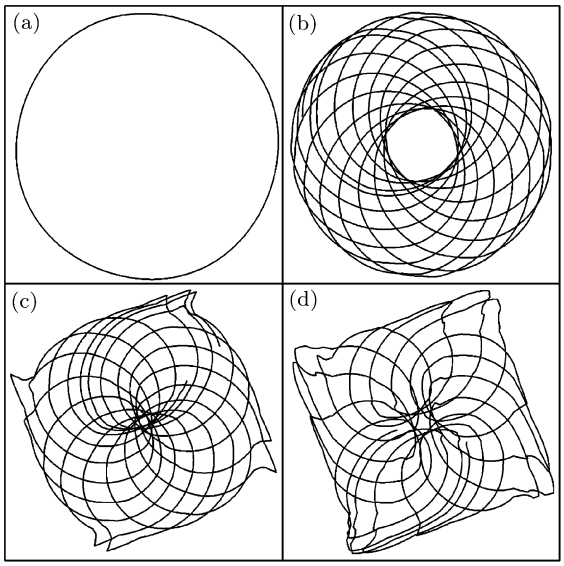



**Fig. 2.** Tip orbits of antispirals for different coupling strengthes of active variable $u$: (a) $D_u = 0.0352$; (b) $D_u = 0.0328$; (c) $D_u = 0.0308$ and (d) $D_u = 0.0280$.

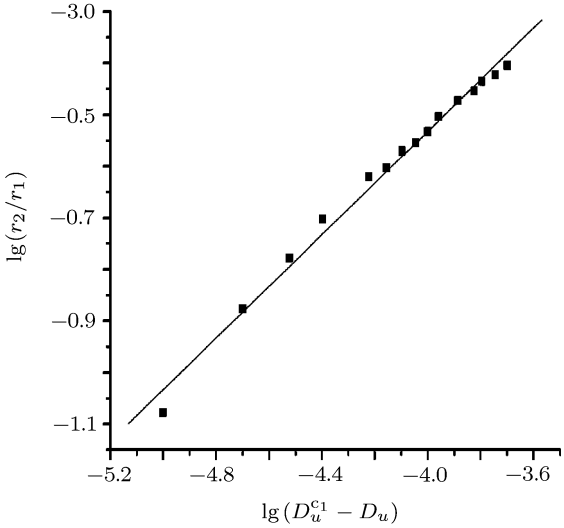



**Fig. 3.** Log–log plot of the amplitude ratio vs distance from the bifurcation point. The fitting line to the 15 testing points close to the transition gives an exponent of $0.49 \pm 0.01$, where the uncertainty is derived from the fitting errors. A supercritical Hopf bifurcation is clearly demonstrated by the data.

The size of the petals of the antispiral tip orbit

increases continuously as the coupling strength $D_u$ decreases. When $D_u$ crosses the second critical value ($D_u^{c_2} \approx 0.0188$), the system undergoes a new transition from meandering antispiral waves to spatiotemporal turbulence. The antispiral wave instability is caused by Doppler effect, and the process of unstabilization is shown in Fig. 4. Figure 4(a) presents the well behaved antispiral at $t = 0$. Because of the Doppler effect, the antispiral tip moves toward to its adjacent waves and compresses them, as shown in Fig. 4(b). When the waves in the antispiral core region are compressed too much and the heterogeneity increases beyond a threshold, waves in this region can collide with each other, and then antispiral waves can break and new defects can be generated (Fig. 4(c)). The newly generated defects drift apart and self-organize into new daughter antispirals which will also meander as the mother antispiral. More wave collisions happen and more defects are generated and the system thus finally fall into spatiotemporal defective turbulence which is shown in Fig. 4(d). This is the first time to show that Doppler instability of defective turbulence can occur for antispirals, and also the first time to show that Doppler instability can occur in oscillatory systems around Hopf bifurcations.

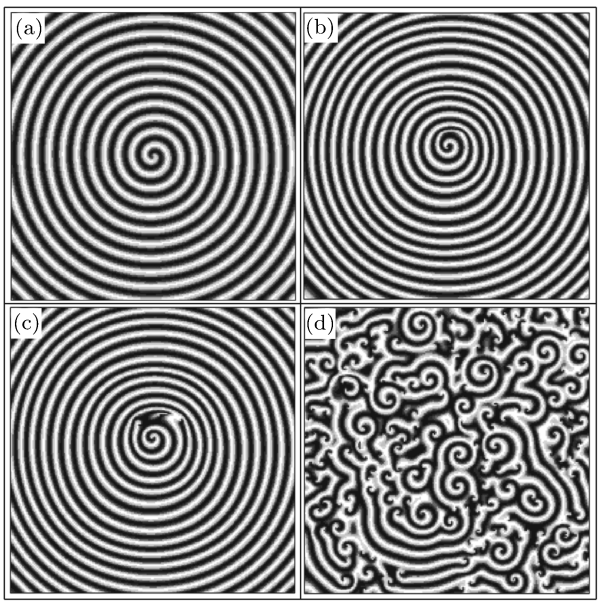



**Fig. 4.** Development of antispiral breakup into turbulence via Doppler instability. $D_u = 0.0128$: (a) $t = 0$; (b) $t = 6800$; (c) $t = 7100$; (d) $t = 8000$.

In order to explain how Doppler effect causes antispiral wave breakup via meander, we investigate the wave dynamics of Eq. (1) in a 1D cable driven by a periodic signal at the left boundary and the No-Flux condition is applied for the right boundary. The driven system reads

$$\begin{aligned}\dot{u}_i &= \frac{1}{\varepsilon}\left(u_i - \frac{u_i^3}{3} - v_i\right) + D_u(u_{i-1} + u_{i+1} - 2u_i) \\ &\quad + \Omega(x)F\sin\left(\frac{2\pi}{T}t\right), \\ \dot{v}_i &= u_i - \sigma v_i + \delta + \gamma D_u(v_{i-1} + v_{i+1} - 2v_i), \end{aligned} \tag{2}$$

where $i = 1, \ldots, 200$. In the simulation of Eq. (2), we select the driven strength $F = 1.0$ and function $\Omega(x) = 1$ at space sites $i = 1, \ldots, 10$, and $\Omega(x) = 0$ otherwise. Figure 5 shows space–time patterns of $u$ for different driven period $T$ in 1D simulations. We find that for large driven period (i.e., small driven frequency) periodic wave trains can be generated from the pacing source and propagate from the right side to the left side (inwardly to the source). This is consistent with the inward propagation of antispiral waves from the boundary to the core centre in 2D simulations. As we decrease the driven period $T$, wave trains also can propagate in the 1D system just with smaller wave numbers (see Fig. 5(a) for $T = 10.00$ and (b) for $T = 2.60$). When the driven period crosses a critical value $T_{\rm Th} = 2.59$, wave propagation stops and the system falls into spatial homogeneous oscillatory state shown in Fig. 5(c). For even smaller driven period, such as $T = 0.10$, the homogeneous oscillatory state remains unchanged, and thus no wave can propagate

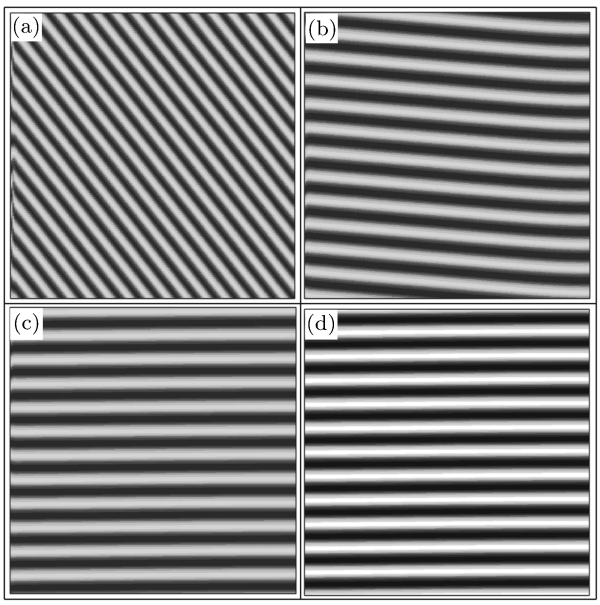



**Fig. 5.** Space–time patterns of $u$ in Eq. (2) for different driven period $T$ with $D_u = 0.0352$: (a) $T = 10.00$; (b) $T = 2.60$; (c) $T = 2.59$; (d) $T = 0.10$. Wave propagation stops after the threshold $T \leq T_{\rm Th} \approx 2.59$.

in this system as shown in Fig. 5(d), either. Therefore, for this 1D system, there exists a minimum driven pe-

riod $T$ for the driven wave source, below which, wave propagation stops. And this propagation stop plays the key role for wave collisions leading to breakup turbulence in 2D system.

Figure 6 shows the actual maximum and minimum periods of the meandering antispiral waves of Eq. (1), and the minimum driven period $T_{\rm Th}$ in the corresponding 1D system (which has been shown in the above paragraphs) is also given for comparison. Here we define the period as the time interval between successive maxima of the variable $u$. The system was run for several thousand periods after a transient. We measure the maximum period ($P_{\max}(i,j)$) and minimum period ($P_{\min}(i,j)$) at all spatial sites in the 2D square sheet. And we select the maximal $P_{\max}(i,j)$ and minimal $P_{\min}(i,j)$ $(i,j=1,\ldots,200)$ as the actual maximum ($T_{\max}$) and minimum ($T_{\min}$) periods of the meandering antispiral waves. When the antispiral is stable and periodic, there exists only a single period for any space site of the system. After the onset of meandering, the period varies in the antispiral core region due to Doppler effect. And the meandering tip can be regarded as a moving wave source for wave trains with periods varying in space and time. When the minimum period of the moving wave source becomes smaller than the minimum driven period of the corresponding 1D system, wave propagation stops in this region. Waves newly emitted from the antispiral core can catch up and collide with them. Then these collision events break waves and new defects are formed. So the antispiral wave instability can be rationalized as follows. With large coupling strength $D_u$, the antispiral is stable and there exists only a unique period. As the coupling strength $D_u$ decreases and crosses the first critical value $D_u^{\rm c_1} \approx 0.0341$, antispiral meanders. Figure 6 thows that the period of the antispiral waves varies and the minimum period decreases as $D_u$ decreases. When the coupling strength $D_u$ becomes smaller than the second critical value ($D_u^{\rm c_2} \approx 0.0188$), the variation of period in the antispiral core region caused by Doppler effect becomes so pronounced that the minimum period of the antispiral is the minimum driven period $D_{\rm Th}$, then wave propagation stops in the given region and Doppler instability induced wave breakup occurs.

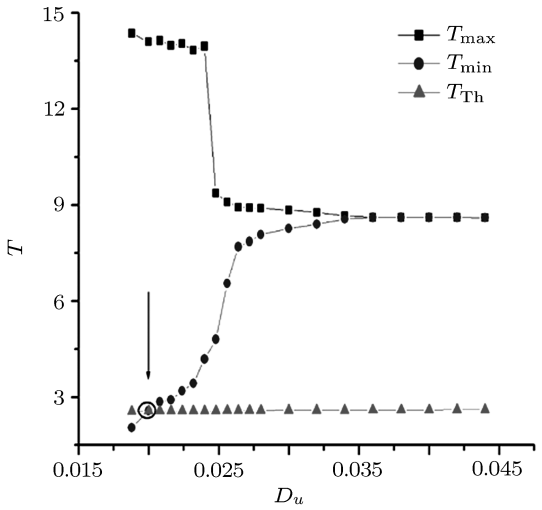



**Fig. 6.** Variations of the maximum (squares) and minimum (circles) periods of antispiral waves in 2D system by varying $D_u$ for the control parameters same as Fig. 1. The variation of the smallest threshold ($T_{\rm Th}$) of the driven period in the corresponding 1D system are represented by triangles. The intersection of curves $T_{\min}$ and $T_{\rm Th}$ ($D_u \approx 0.0200$) predicts the transition from meandering antispiral to spiral turbulence in 2D system ($D_u^{\rm c2} \approx 0.0188$) with a fairly good precision.

## 4. Summary and discussion

In conclusion we have investigated antispiral wave breakup in a discrete oscillatory reaction–diffusion system (FHN model) via Hopf bifurcation. The system has two critical values. With high coupling strength $D_u$, a stable antispiral wave can be formed and its tip moves in a small circle. As the coupling strength $D_u$ decreases, acrosses the first critical value, the stable antispiral wave undergoes a transition to meander and then the period of the antispiral varies due to the Doppler effect. By measuring the amplitude ratio for compound inward rotations, we have clear evidence that a supercritical Hopf bifurcation gives rise to this meandering. When $D_u$ decreases across the second critical value, the variation of the period in the antispiral core region caused by the Doppler effect became so pronounced that the antispiral wave breakup into spatiotemporal turbulence occurs. Our findings suggest that Doppler instability can be observed not only in continuous excitable media for normal spirals, in discrete oscillatory reaction–diffusion media antispirals can also develop defective turbulence via the Doppler instability mechanism.

# References


[1] Winfree A T 1987 *When Time Breaks Down* (Princeton: Princeton University Press)

[2] Kapral R and Showalter K 1995 *Chemical Waves and Pattern* (Dordrecht: Kluwer)

[3] Murray J 1989 *Mathematical Biology* (Berlin: Springer)

[4] Yamada T and Kuramoto Y 1976 *Prog. Theor. Phys.* **55** 2035

[5] Selpuchre J A, Dewel G and Babloyantz A 1990 *Phys. Lett.* A **147** 380

[6] Vanag V K and Epstein I R 2001 *Science* **294** 835

[7] Vanag V K and Epstein I R 2001 *Phys. Rev. Lett.* **87** 228301

[8] Vanag V K and Epstein I R 2002 *Phys. Rev. Lett.* **88** 088303

[9] Gong Y F and Christini D J 2003 *Phys. Rev. Lett.* **90** 088302

[10] Brush L, Nicola E M and Bär M 2004 *Phys. Rev. Lett.* **92** 089901

[11] Nicola E M, Brush L and Bär M 2004 *J. Phys. Chem.* B **108** 14733

[12] Cao Z J, Zhang H and Hu G 2007 *Europhys. Lett.* **79** 34002

[13] Cui X H, Huang X Q, Cao Z J, Zhang H and Hu G 2008 *Phys. Rev.* E **78** 026202

[14] Shao X, Wu Y B, Zhang J Z, Wang H L and Ouyang Q 2008 *Phys. Rev. Lett.* **100** 198304

[15] Cross M C and Hohenberg P C 1993 *Rev. Mod. Phys.* **65** 851

[16] Barkley D, Kness M and Tuckerman L 1990 *Phys. Rev.* A **44** 2489

[17] Bär M and Eiswirth M 1993 *Phys. Rev.* E **48** 1635

[18] Li G, Ouyang Q, Petrov V and Swinney H L 1996 *Phys. Rev. Lett.* **77** 2105

[19] Ouyang Q, Swinney H L and Li G 2000 *Phys. Rev. Lett.* **84** 1047

[20] Tobia S M and Knobloch E 1998 *Phys. Rev. Lett.* **80** 4811

[21] Zhou L Q and Ouyang Q 2000 *Phys. Rev. Lett.* **85** 1650

[22] Sandstede B and Scheel A 2000 *Phys. Rev.* E **62** 7708

[23] Aranson I S and Kramer K 2002 *Rev. Mod. Phys* **74** 99

[24] Weiss J N, Karagueuzian H S, Qu Z L and Chen P S 1999 *Circulation* **99** 2819

[25] Bär M and Guil M O 1999 *Phys. Rev. Lett.* **82** 1160

[26] Yang J Z, Xie F G, Qu Z L and Garlinkel A 2003 *Phys. Rev. Lett.* **91** 148302

[27] Xie F G, Xie D Z and Weiss J N 2006 *Phys. Rev.* E **74** 026107

[28] FitzHugh R A 1961 *Biophys. J.* **1** 445